Nuclear Engineering and Technology 53 (2021) 1436–1445

Contents lists available at ScienceDirect

Nuclear Engineering and Technology

journal homepage: www.elsevier.com/locate/net

Original Article

# A study on the dynamic characteristics of the secondary loop in nuclear power plant

J. Zhang [a, b], S.S. Yin [c], L. Chen [a, b], Y.C. Ma [a, b], M.J. Wang [a, b], H. Fu [a, b], Y.W. Wu [a, b], W.X. Tian [a, b], S.Z. Qiu [a, b], G.H. Su [a, b, *]

[a] Shaanxi Key Lab. of Advanced Nuclear Energy and Technology, Xi'an Jiaotong University, Xi'an, 710049, China
[b] Department of Nuclear Science and Technology, State Key Laboratory of Multiphase Flow in Power Engineering, Xi'an Jiaotong University, Xi'an, 710049, China
[c] Science and Technology on Reactor System Design Technology Laboratory, Nuclear Power Institute of China, Chengdu, China

ARTICLE INFO

*Article history:*
Received 26 April 2020
Received in revised form
9 October 2020
Accepted 15 November 2020
Available online 27 November 2020

*Keywords:*
Dynamic characteristics
The secondary loop
Turbine
Condenser

ABSTRACT

To obtain the dynamic characteristics of reactor secondary circuit under transient conditions, the system analysis program was developed in this study, where dynamic models of secondary circuit were established. The heat transfer process and the mechanical energy transfer process are modularized. Models of main equipment were built, including main turbine, condenser, steam pipe and feedwater system. The established models were verified by design value. The simulation of the secondary circuit system was conducted based on the verified models. The system response and characteristics were investigated based on the parameter transients under emergency shutdown and overload. Various operating conditions like turbine emergency shutdown and overspeed, condenser high water level, ejector failures were studied. The secondary circuit system ensures sufficient design margin to withstand the pressure and flow fluctuations. The adjustment of exhaust valve group could maintain the system pressure within a safe range, at the expense of steam quality. The condenser could rapidly take out most heat to avoid overpressure.



## 1. Introduction

Nuclear power system features strong reliability, economy and environmental friendliness. The pressurized water reactor comprises two circuits, both require higher safety. The coolant system of primary loop transports fission heat from reactor core to the secondary side of steam generator, thus saturated steam generates. The second loop system has two functions: first, forming a closed thermodynamic cycle, the generated steam is sent to the steam turbine and relevant mechanical equipment for work, realizing the energy transition among thermal energy, mechanical energy and other energy forms (such as electric energy); Second, the second circuit takes away the heat energy from the reactor fission to ensure the reactor safety.

The secondary circuit system of nuclear power plant consists of several power machinery, where a series of equipment such as feedwater system and steam discharge system, various control valves, safety valves participate in the heat discharge. (Fig. 1). The flow process of working fluid is as follows: driven by large pressure difference, the superheated steam generated by steam generator runs into the main steam turbine for work, afterwards the spent steam is discharged into the condenser, which is stored in the hot well; a large amount of steam is directly discharged into the condenser during emergency transients; the condensation is pumped and pressurized into the water supply system and then enters the steam generator. Therefore the flow and thermal procedure in the secondary circuit system is completed. The condenser, acts as the cold end, takes out the heat of the low-quality exhaust steam from the circulation system.

Nuclear power systems concerns on safety and extensive evaluations under accident conditions have been conducted [1,16,17]. Acting as power system, the reliability and economy of the second circuit directly affect the reliability and economy of nuclear power plant; besides, various operating conditions and typical accidents are also tightly related to the reactor safety. Therefore, establishing dynamic models of the second circuit model and analyzing the

* Corresponding author. Shaanxi Key Lab. of Advanced Nuclear Energy and Technology, Xi'an Jiaotong University, Xi'an, 710049, China.
*E-mail addresses:* ghsu@xjtu.edu.cn, ghsu@mail.xjtu.edu.cn (G.H. Su).

https://doi.org/10.1016/j.net.2020.11.014

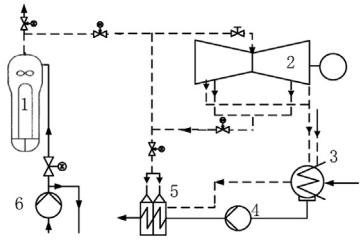


1.Steam Generator 2.Turbine 3.Condenser 4.Condensate pump 5.Ejector 6.Feedwater pump

**Fig. 1.** Structure of secondary system.

operation characteristics under various transient conditions are of great significance in nuclear power plants design, operation procedure development and automatic control strategies. The second loop system, employed as a heat sink, is related to the operating transients and decides the heat output capability from primary loop. More relevant studies are necessary [1–3].

In the engineering field, higher reliability requirements focus on the thermal system simulation of nuclear power [4]. The widely application of dynamic model in system simulation is getting closer to reality, which meet the needs in real-time and interactivity. It features the characteristics of economy, convenience, flexible modification, repeated testing and safety. Mathematical modeling were employed for thermal system simulation. A variety of simulation software were introduced for engineering and safety analysis [5–7] such as ISAS, CATHARE, TRAC, RELAP, RETRAN, GSE, APROS, covering nuclear control system design and optimization, plant operating characteristic diagnose and improvement, start-stop strategy, reactor and turbine lifetime analysis, accident analysis and prediction, operation procedures development and accident handling solution, and system reliability analysis. While the simulation of second circuit needs improving. For instance, based on the basic equations of RELAP5 hydraulic model in order to solve with other hydraulic models, the turbine model in RELAP5 ignores the complex structure inside the turbine and the specific fluid flow in the stage and fails to accurately reflect dynamic operation characteristics. Therefore the prediction precision decrease for transient condition and several studies [8] were conducted on the RELAP modification to improve the accuracy. Compared with the vigorous development of training simulators, simulation systems for engineering needs more efforts.

In this study, the dynamic mathematical models of the main equipment in secondary circuit system are established for nuclear power plant. The second loop system simulation analysis program is developed, focusing on the dynamic characteristics of second loop system under various variable conditions. The system models could be employed alone for the simulation analysis of secondary loop, and could also be applied as the extension and supplement for full system simulation. The mathematical models of the second loop system, including steam turbine, condensing equipment, steam piping system and water supply system, are established. Moreover, the model precisions of main equipment are proved and simulation tests are carried out. Therefore the simulation and analysis of the second loop system are performed to verify the dynamic response ability under transient conditions of engineering application.

## 2. Basic dynamic model

### 2.1. Flow and thermal models

The system decomposition and simplification were conducted according to the thermal system characteristics. Firstly, the complex large system was decomposed into steam turbine system, condensing equipment, steam pipeline and the water supply system. Secondly, to solve the system stiffness, the process was divided into fluid flow, heat transfer and mechanical energy transfer. Thirdly, the lumped parameterization was applied to large volumetric devices, mathematical model is simplified into ordinary differential form. Thus the fluid thermodynamic parameters are linearly distributed along control bodies [9], with the averaged change rate of state parameter at exit. The mathematical-physical models were built for working fluid, the equations of mass conservation, momentum conservation, energy conservation, thermodynamic state equation, physical property and heat transfer equation were established. Therefore the closed differential equation and algebraic equation system are established.

The fluid state in the secondary circuit includes steam and condensate. Condense processes of compressible and incompressible fluid were both considered. A modular modeling method was applied to compressible fluid, and the fluid network modeling method was employed for incompressible fluid.

1) Modules modeling for compressible fluid

Modular modeling of compressible fluid, which is a hierarchical modeling method, divides the thermal system into different devices and modules according to energy conversion. The internal state parameters of module are lumped parameterized, and various modules are connected to form thermal equipment. The modularity shows independence from other modules [10], thus separate module replacement and modification could improve model reusability.

According to the conservation equations, the mass and energy conservation equation of fluid flow show the storage of mass and energy; the momentum conservation equation indicates the flow resistance. The storage and resistance characteristics are represented by a flow storage type module (S type) and a flow resistance type module (R type), respectively. The storage module is

$$\begin{cases} \dfrac{dp}{dt} = \dfrac{G_E - G_L}{V\partial\rho/\partial p} - \dfrac{\partial\rho}{\partial h}\Big/\dfrac{\partial\rho}{\partial p}\dfrac{dh}{dt} \\ \dfrac{dh}{dt} = \dfrac{(G_E h_E - G_L h_L) + Q + \left(h - \dfrac{1}{\partial\rho/\partial p}\right)(G_L - G_E)}{V\left(\rho + \dfrac{\partial\rho}{\partial h}\Big/\dfrac{\partial\rho}{\partial p}\right)} \\ p_L = p_E = p \end{cases} \tag{1}$$

Ignoring the mass and energy equation and time constant of momentum accumulation, the flow resistance module is deduced by

$$G_E = \lambda\sqrt{\rho(p_E - p_L)} \tag{2}$$

Moreover, the pressure and flow show bidirectional transfer characteristics. In order to ensure the module connection, the connection should only exist between R-type module and *S*-type module.

(2) Fluid network modeling of incompressible fluids

Incompressible fluids only consider the pressure drop, which applies to the water supply system. These piping systems feature complex network topologies, while only parameters at each node were concerned instead of the internal flow mechanisms. Therefore, the pipeline system was abstracted into a fluid network to solve coupling pressure and branch flow rate at nodes. Therefore

these parameters could only be obtained by the downstream boundary conditions: the flow rate of inflow and outflow at any node was zero; the algebra sum of differential pressure is zero for each branch in closed loop. The equation group of the entire network is closed, the node pressure and branch flow were obtained.

### 2.2. Mechanical energy transfer model

The mechanical energy transfer process adopts the modules of torque storage and rotational resistance. Torque storage modules are commonly used to simulate angular momentum accumulation in rotating components, such as the rotor inertia of turbine. The sum of rotational inertias on rotating shaft should be considered, which is expressed as follows [11]:

$$d\omega / dt = \left(M_{turb} - M_{gen} - M_{mech.loss}\right) / \left(I_{turb} + I_{gen}\right) \quad (3)$$

where $M_{turb}$, $M_{gen}$ and $M_{mech.loss}$ denote turbine torque, generator torque and mechanical loss torque. $I_{turb}$and$I_{gen}$represent the rotational inertia of turbine and generator, respectively. Depending on the characteristics of various devices such as pump, generator and gearbox, the rotating resistance module was obtained by their respective characteristics or empirical curves.

### 2.3. Program flow chart

The basic module library and device model library were packaged and unified interface were adopted. The program structure and calculation process are shown in Fig. 2. The Gear method was adopted to solve rigid differential equations of this system. Solving the large time deviation for different thermal system, the Gear method has the advantages of automatic variable step size and order, fast calculation speed and stable solution. In addition, the Monte Carlo method was used to solve algebraic equations.

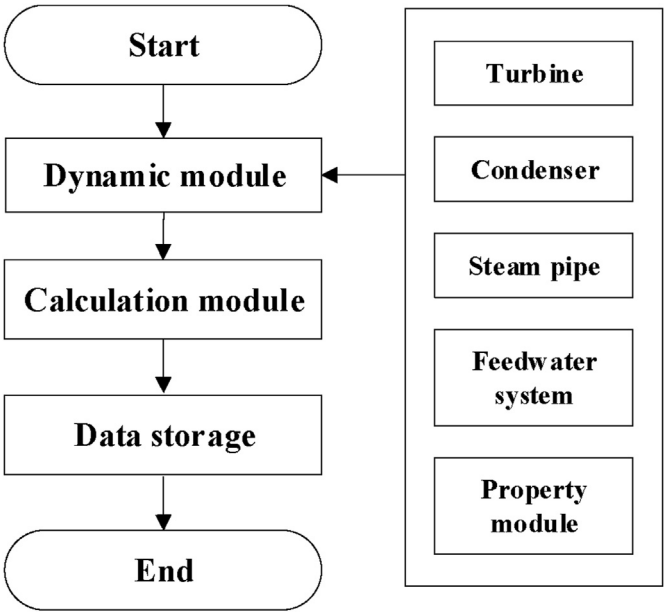


**Fig. 2.** Program structure and Flow chart.

## 3. Component modeling

### 3.1. Models of turbine

The steam turbine, a high-speed rotating machine with steam as working medium, converts thermal energy into mechanical energy for power supply, feedwater pump and circulating pump. Its simulation and characteristics are of great significance to the secondary circuit system Fig. 3. The steam turbine consists of main steam valve, regulating valve, and regulating stage. The steam turbine module includes flow resistance type module (valve, regulating stage and non-regulating), flow storage module (chambers of valve, regulating stage and non-regulating stage) and torque storage module (turbine rotor). The flow resistance module describes the flow variation caused by pressure; the flow storage module describes the volume inertia due to mass and energy storage; and the torque storage module describes the torque inertia of rotation axis. It should be ensured that the resistance module and storage module connect to each other. Different combinations of basic modules describe various types of steam turbine models, such as feed pump steam turbines, reverse steam turbine cycle pump steam turbines.

#### 3.1.1. Models for flow resistance

1) Steam valve

The steam valve module, which is a universal valve for compressible fluids, could be used to model main steam valve and adjusting valve. Isentropic process is assumed and the flow rate is calculated by the inlet and outlet pressure difference. Ignoring the storage characteristic, there are:

$$G_E = G_L = k_{mx} k_v (1 - 0.367X / X_{cr}) \sqrt{\rho_E p_E X} \quad (4)$$

$$h_L = h_E \quad (5)$$

where $G_E$ is the inlet flow rate, $kg \cdot s^{-1}$; $\rho_E$ is the inlet steam density, $kg \cdot m^{-3}$; $p_E$ is the inlet pressure, Pa; $X$is the pressure loss coefficient; $X_{cr}$is the critical pressure loss; $k_v$ is the valve characteristic coefficient, related to the valve opening; $k_{mx}$ is the valve correction factor, related to the maximum valve area; $G_L$ is the outlet flow rate, $kg \cdot s^{-1}$; $h_L$ and $h_E$ are the outlet and inlet enthalpy, $J \cdot kg^{-1}$, respectively.

2) Regulating stage

The regulating stage includes contraction nozzle and moving

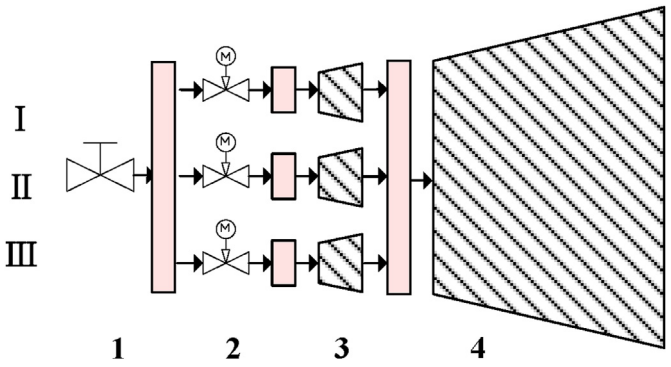


**Fig. 3.** Typical turbine structure.

blade (Fig. 4). The initial steam velocity $C_0$ is assumed to be zero; the regulating stage has the reaction $\Omega = 0$, with pressure difference of zero.

The flow rate of nozzle $G_{rs}$, equals to the flow rate of regulating stage, is

$$G_{rs} = \mu G_{crt} = 0.648\mu A_1 \sqrt{p_0/v_0}\ \varepsilon \le \varepsilon_{cr} \tag{6}$$

$$G_{rs} = \mu\sqrt{1 - [(\varepsilon_1 - \varepsilon_{cr})\ /\ (1 - \varepsilon_{cr})\ ]^2}G_{crt}\ \varepsilon > \varepsilon_{cr}$$

where $\mu$ is a flow rate coefficient (0.96–0.98), $\varepsilon$ and $\varepsilon_{cr}$ are the pressure ratio and the critical pressure ratio, respectively.

The relative velocity at blade inlet ($W_1$/m·s$^{-1}$) and outlet ($W_2$/m·s$^{-1}$) are

$$W_2 = \varphi W_1 = \varphi\sqrt{C_1^2 + \left(\frac{n\pi d_{cp}}{60}\right)^2 - 2\frac{n\pi d_{cp}}{60}C_1\cos\alpha_1} \tag{7}$$

where $d_{cp}$ is the averaged diameter/m, $n$ is the turbine speed/r·min$^{-1}$; $\varphi$ is the cascade speed coefficient.

Based on velocity triangle of the absolute velocity at blade outlet,$C_2$/m·s$^{-1}$, The power, $\Delta h_u$/J·kg$^{-1}$, is

$$\Delta h_u = 0.5\left(C_1^2 - W_1^2 + W_2^2 - C_2^2\right) \tag{8}$$

The power loss in the regulating stage includes fan loss, $\Delta h_\theta$; friction loss, $\Delta h_f$; impact loss, $\Delta h_i$; windage loss, $\Delta h_w$ and segment loss, $\Delta h_e$. The expression are as follows:

$$h_L = h_0 - \Delta h_u + \Delta h_\theta + \Delta h_f + \Delta h_i + \Delta h_w + \Delta h_e \tag{9}$$

The work $P_{rs}$ and internal efficiency $\eta_i$ are

$$P_{rs} = G_{rs}(h_0 - h_2) \tag{10}$$

$$\eta_i = (h_0 - h_2)\ /\ h_0 - h_{1t} \tag{11}$$

3) Non-regulating stage

The non-regulating stage module, a universal module, could simulate the entire working stage of the multi-stage steam turbine and the intermediate stage of a steam extraction turbine.

The flow rate of the non-regulating stage is

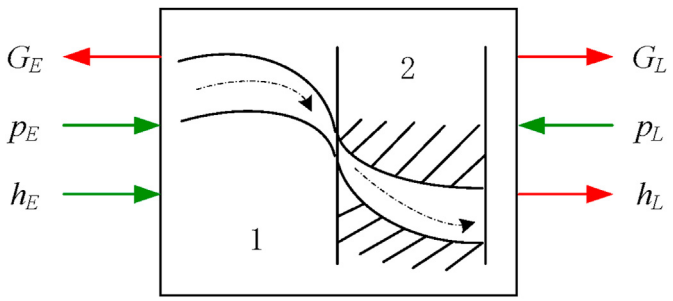


1. Nozzle 2. Blade

**Fig. 4.** Regulating stage module.

$$\frac{G_E}{G_{E0}} = \sqrt{\frac{p_E^2 - p_L^2}{p_{E0}^2 - p_{L0}^2}}\sqrt{\frac{T_{E0}}{T_E}}\sqrt{1 - 0.4\frac{\Delta n}{n_0}} \tag{12}$$

where $G_{E0}$ is the rate flow/kg·s-1 ; $p_{E0}$ is the rate inlet pressure/Pa; $T_{E0}$ is the rated inlet temperature/K; $n_0$ is the rated rotational speed/r·min$^{-1}$; $\Delta n$ is the rotational speed variation/r·min$^{-1}$; $p_{L0}$ is the rate outlet pressure of non-regulating stage/Pa; $p_L$ is the outlet pressure of non-regulating stage/Pa.

The internal efficiency of the non-regulating stage is

$$\frac{\eta_i}{\eta_{i0}} = \frac{n}{n_0}\sqrt{\frac{\Delta h_{t0}}{\Delta h_t}}\left(2 - \frac{n}{n_0}\sqrt{\frac{\Delta h_{t0}}{\Delta h_t}}\right) \tag{13}$$

where $\eta_{i0}$ is the rated internal efficiency, $\Delta h_{t0}$ is the rated enthalpy drop/kJ·kg$^{-1}$; $\Delta h_t$ is the rated enthalpy drop/kJ·kg$^{-1}$; $n$ is the rotate speed/r·min$^{-1}$.

The outlet enthalpy and work of non-regulating stage are respectively

$$h_L = h_E - \Delta h_t \eta_i \tag{14}$$

$$P_t = G_E(h_E - h_L) \tag{15}$$

*3.1.2. Storage models for flow torque*

Due to the small steam volume in the turbine, $u = h$ is assumed and the influence of the enthalpy on pressure is ignored. The conservation equations of mass, energy and momentum in Eq. (1) were simplified.

For multi-inlet storage modules such as steam chamber of regulating stage, the flow rate is the sum of each branch and the inlet enthalpy is averaged. Besides, the turbine rotor module has much larger moment of inertia than its linking equipment (such as propellers, pumps, generators, etc.). Therefore it exhibits stronger torque storage characteristics [12].

The turbine power $P$/kW and internal efficiency are

$$P = G_L(h_E - h_L) \tag{16}$$

$$\eta_{it} = (h_L - h_E)\ /\ \Delta h_t \tag{17}$$

The rotational speed $n$/r·min$^{-1}$ is

$$dn\ \Big/\ dt = 900\left(P - P_f\right)\Big/\pi^2 J_t n \tag{18}$$

*3.2. Models of condenser*

*3.2.1. Condenser*

A single-shell, double-flow, surface-type condenser was simulated. The basic structure is shown in Fig. 5. The condenser structure should meet the load and vacuum requirements of the secondary circuit system. The condenser was divided into the shell side and the tube side: The cooling water was driven by circulating water pump on the pipe side, and the steam was condensed outside the pipe. Thus the heat was transferred to the cooling water through pipe wall, and continuous cooling water circulation maintains high vacuum.

The condenser dynamic model is established based on the following assumptions: the condenser model adopted the lumped parameters, employing a uniform value of the inlet pressure; the

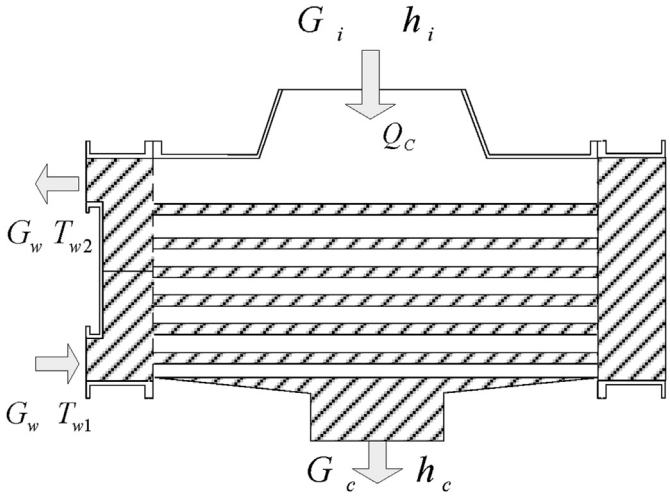


**Fig. 5.** Typical condenser module.

two-phase working fluid is saturated using homogeneous model; the wall temperature variation is consistent with that of the working fluid at shell side; the temperature variation at outlet was adopted for the whole condenser.

As a type of shell-and-tube heat exchanger, the heat exchange process of condenser includes: steam condensation at shell side, convective heat transfer of cooling water in pipe side, and heat conduction through pipe wall. Heat dissipation are ignored [13].

Ths heat balance equation is [14].

$$Q_c = kA\Delta T_m = G_w c_w (T_{w2} - T_{w1}) \tag{19}$$

where $Q_c$is the condensation heat/kW; $k$is the overall heat transfer coeffcient/kW·(m2·°C)-1, where the Berman formula is used ; $A$ is the condensation area/m2 ; $\Delta T_m$ is logarithmic mean temperature difference/°C ; $G_w$ is the flow rate of cooling water/kg·s-1 ; $c_w$ is the specific heat of cooling water/kJ·(kg·°C)-1 ; $T_{w1}$ is the inlet temperature of cooling water/°C.

Under normal conditions, the total condensation pressure $p_c$ as a function of the steam condensation temperature $T_s$, is almost equal to the vapor partial pressure $p_s$,

$$T_s = T_{w1} + 520 \Big/ m + \Delta T \Big/ \left[e^{AK/(4.187G_w)} - 1\right] \tag{20}$$

where the cycle magnification $m$ is the ratio of cooling water flow rate $G_w$ to condenser load $G_c$, ranging between 50 and 120.

The transient model of condenser is categoried as shell side and tube side. Both steam zone and air zone were considered The condenser pressure, $p_c = p_s + p_a$. The concerned parameters include the condenser water level $h$, hot well water enthalpy value $h_{hw}$, outlet temperature of cooling water $T_{w2}$, and subcooling degree of condensed water $\Delta T_n$, etc.

(1) shell side

For steam zone of shell side, the pressure of the condenser vapor zone is based on a two-phase lumped parameter dynamics model. The saturated enthalpy of liquid $h'$ , saturated enthalpy of vapor phase $h''$, and the saturated temperature $T_s$ are the function of two-phase pressure $p(t)$, which varies with time.

The pressure equations of steam pressure are deduced

$$\frac{dp_s}{dt} = \frac{\sum (Gh)_i - Q_c - (\rho' h' - \rho'' h'')/(\rho' - \rho'') \sum G_i}{\varepsilon' V' + \varepsilon'' V'' - V + c_m \phi_m m_m dT_s/dp} \tag{21}$$

The change rate of water level is

$$\frac{dH}{dt} = \frac{\sum G_i}{A_{hw}(\rho' - \rho'')} - \frac{V' d\rho'/dp + V'' d\rho''/dp}{A_{hw}(\rho' - \rho'')} \frac{dp_s}{dt} \tag{22}$$

where $A_{hw}$ is the heat transfer area of heat sink/m.$^2$

For the air zone of shell side, tiny non-condensing gas comes from vacuum equipment leakage, hydrophobicity and hydration during normal operation, most of which is air. The pressure of air is

$$V dp_a / dt = R_a (T_a + 273) dm_a / dt \tag{23}$$

where $m_a$ is the mass of air/kg; $R_a$is the air constant/J·(kg·°C)$^{-1}$, set as 287.05; $T_a$is the average temperature of air/°C.

(2) tube side

As to the tube side during normal operating conditions, the hot water level is below the tube bundle in condenser. While the condensing tube bundle is submerged under certain abnormal conditions. Hence the model of condenser tube includes two parts: bare tube bundle and submerged tube bundle. The inlet and outlet cooling water temperature is expressed as $T_{w2L}$ and $T_{w2Y}$. The metal tube wall of bare and submerged tube bundle are divided into the shell side and tube side, respectively.

For the bare tube bundle, the equation for the cooling water outlet temperature is

$$dT_{w2L} / dt = [Q_c - c_w G_{wL} (T_{w2L} - T_{w1})] / c_w m_{wL} \tag{24}$$

where $m_{wL}$ means the mass of cooling water/kg, and $G_{wL}$ denotes the flow rate of cooling water/kg·s$^{-1}$.

The cooling water outlet temperature of the submerged bundle is obtained:

$$dT_{w2Y} / dt = [Q_w - c_w G_{wY} (T_{w2Y} - T_{w1})] / (c_w m_{wY} + c_m m_{mY}) \tag{25}$$

$$Q_w = \lambda_w \Big/ d_1 \cdot 0.023 \mathrm{Re}^{0.8} \mathrm{Pr}^{0.4} A_Y (T_{hw} - T_{wA}) \tag{26}$$

where $M_{wY}$ is the mass of cooling water/kg, $M_{mY}$ is the mass of metal tube/kg, $G_{wY}$ is the flow rate ofcooling water/kg·s$^{-1}$, $Q_w$ is the convective heat transfer/kW, $A_Y$ represents the heat transfer area of submerged tubes/m$^2$,$T_{hw}$ is the heat sink temperature/°C, $T_{wA}$ denotes the averaged cooled water/°C; where $\lambda_w$ means the heat transfer coefficient of cooling water/W·(m·°C)$^{-1}$, $d_1$ is the inner diameter/m。

(3) condensed water subcooling

Subcooling degree of condensed water is an important indicator of turbine operating. Greater subcooling degree takes away more heat and lower the economics; larger subcooling degree increases the oxygen content, thus affecting the long-term operation reliability of the unit. Several reasons might introduce higher subcooling degree: air accumulation caused by leakage or vacuum system fault, submerging condensing tube bundle due to water level adjustment failure, and the structural defects in tube bundle and ejector arrangement;

Heat sink enthalpy is

$$dh_{hw}/dt = (\varepsilon' V' dp_s/dt - Q_w)/V'\rho' \tag{27}$$

#### 3.2.2. Ejector

The ejector extracts the non-condensing gas to maintain the vacuum degree and heat transfer, as shown in Fig. 6. The high-speed steam enters the nozzle and exchanges momentum with surrounding gas in the mixing chamber, thus a high vacuum achieves. Afterwards the air-steam mixture is continuously entering the diffuser tube, slowing down the steam speed and increasing the pressure.

The ejector model is based on the following three assumptions: the axial velocity of the fluid is negligible, the pressure field in the mixing chamber is uniform, the friction resistance could be ignored in the diffuser tube.

Semi-empirical formula is applied to calculate the shooting coefficient of ejector:

$$u = \frac{0.652(1/Ma_1 + Ma_1)\frac{p_4}{p_k} - 0.625\frac{p_4}{p_k}\xi - \frac{p_4}{p_0}\frac{A_1}{A_{cr}}}{1.27p_4/p_k - 0.95} \tag{28}$$

where $\xi$ ranges from 0 to 0.05, $p_0$ is the pressure at nozzel inlet/Pa, $p_4$ is the back pressure of ejector/Pa , ranging form 1.0 to 1.1 ; $p_k$ is the averaged pressure/Pa, $Ma_1$ is the steam expansion in the nozzle.

The inlet flow rate of ejector is

$$G_{mix} = u0.648A_{cr}\sqrt{p_0 v_0} \tag{29}$$

where the critical pressure $A_{cr}$ is related to the adiabate coeffcient $K_{1m}$ and $Ma_1$.

### 3.3. Models of steam pipe

As to the steam pipe modeling, the lumped parameter method was used with ordinary differential equation to approximate the parameter distribution characteristics. The complex steam piping system was divided into several sections. Each pipe was established separately based on mathematical models of mass, momentum and energy conservation equations. The characteristics of steam pipeline system are firmly related to the dynamic response of secondary circuit system. The physical phenomena of the steam pipeline simulated in this study were pressure drop, inertia, energy and mass storage, fluid expansion in the pipeline.

Conservation equations for the mass, energy and momentum equations for compressible single-phase fluid were established [15], as elaborated in the in section 2.1.

### 3.4. Models of feedwater system

Thermal fluid network was applied to modeling the water supply system, which mainly simulates the transient characteristics of pressure and flow rate. Ideal incompressible fluid was assumed and heat exchange with environment is ignored.

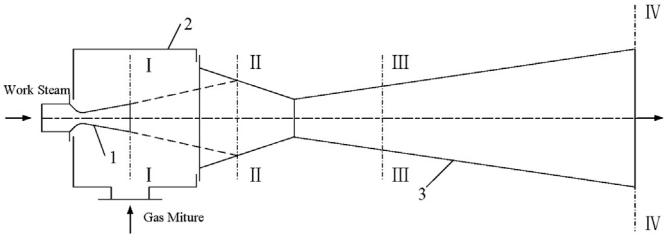


**Fig. 6.** Typical structure of ejector.

Neglecting the heat and mass storage, heat transfer, gravity and friction, the basic equations of the regulating model is obtained. The pressure drop $\Delta p_{cv}$ is related to the valve opening $S_t$.

Centrifugal pump as adopted in this study for feedwater system. The motor connected to the shaft drives the impeller rotating at a high speed, thus the fluid is transferred. Both a series and parallel combination of pumps could be applied to achieve desired flow rate and pressure. Both condensate pump and feed water pump were considered: the condensate pump draws the condensate from hot well to the feed pump; the feed water pump pressurizes the condensate into the steam generator.

The pump curve for head and flow rate is

$$H_t = \frac{H_{t\infty}}{1+k_P} = \frac{u_2}{(1+k_P)g}\left(u_2 - \frac{Q_t}{A_2}\cot\beta_2\right) \tag{30}$$

where $Q_t$is the volume flow rated/m3·s-1 ; $A_2$ is the effective flow area of blade/m2; $d_2$ is the outer diameter/m ; $b_2$ is the blade pitch/m; $\phi_2$ is the discharge coefficient at outlet; $k_P$ is the blade coefficient, ranging from 0.25 to 0.45.

The power of pump

$$\eta = P_t/P = \rho g Q_t H_t/P = \eta_V \eta_h \eta_m \tag{31}$$

where the pump efficiency ($\eta$) is the ratio of idea power P to shaft power, $\eta_V$ is the volume efficiency, $\eta_h$ is the hydraulic efficiency; $\eta_m$ is the mechanic efficiency, all the three are the function of relative rotating speed.

Therefore, the actual curve of H-Q was obtained: First, calculate the $\eta_V$ and $\eta_h$ by assuming an initial $n_s$, thus the idea curve of $H_t - Q_t$ is obtained; afterwards the $H - Q$ curve is obtained and the $n_s$ is updated. The iteration is terminated with a satisfying error of the $n_s$, and the $\eta_m$ is obtained.

The pressure loss of incompressible fluid $\Delta p_{wp}$ consists of the friction pressure drop$\Delta p_l$ and the local pressure drop $\Delta p_c$. According to the principle of thermodynamics, pressure and flow feature two-way transmission, which shows a network characteristic in a thermal system. And the three non-linear equations with three unknowns were solved by the Monte Carlo method.

## 4. Simulation results

The system equipment includes main steam turbine, condensing equipment, steam pipeline system and water supply system. As elaborated above, each sub-system was modeled separately for maintenance. Variables of thesed system were obtained by solving differential equations, using GEAR algorithm. The data input and output interfaces are convenient for observing parameter changes, and reserved physical interfaces facilitate system expansion. The model prediction of main equipment like turbine and condenser were compared with the design parameters. Two extreme operating conditions of emergency stop and overspeed were considered to verify the reliability of the secondary circuit system, where the transient response of parameters were captured.

There are two boundary conditions in the secondary circuit system: the cold-end parameters and the steam system inlet. For storage module, the flow boundary was adopted, as shown in Fig. 7; For resistance module, the pressure boundary was employed and the header J0 was removed.

The flow resistance module (R type) and flow storage module (S type) of the steam pipeline were separately established, and the combination of R and S modules was used to establish the steam pipeline system. In addition, the steam header module and the

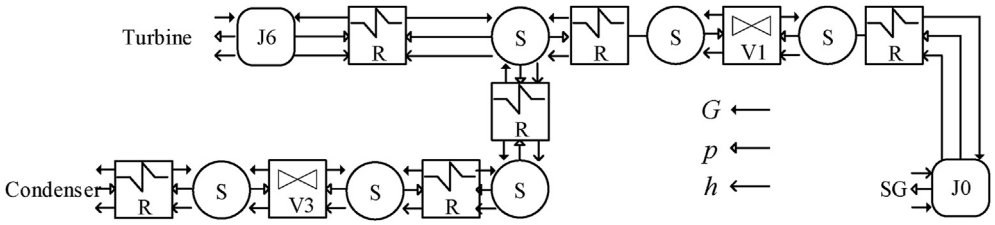


**Fig. 7.** System diagram of secondary circuit.

steam valve module were also included. The interface parameters are shown in the following Table 1.

### 4.1. Models validation

The model predictions were compared with the design value (Dai et al., 2013), where reasonable results were obtained. From Table 2, calculated values which agree well with the design value can be obtained, proving the precision of the main models in this study. Based on the verified model, the system response under emergency shutdown and overload conditions were analyzed next.

### 4.2. System emergency shutdown

The emergency shutdown requires quick response of main steam valve, and the steam should be quickly discharged into condenser to avoid overpressure. The valve control strategy of steam exhaust system is to open a small valve first and then open the other two valve.

(1) Pressure boundary

From Fig. 8(a), The inlet flow rate tends to be balanced after fluctuation. As shown in Fig. 8(b) the flow rate of the steam discharge valve increases rapidly with valve opening. The flow rate of the steam turbine shows a slow trend and afterwards this trend speeds up. In turn, it is required that the control strategy of the steam exhaust system should not cause excessive disturbance.

The pressure, power and flow rate rapidly decrease with the main steam valve shutting down, causing the increase of enthalpy (Fig. 9).

Because a large amount of steam is directly discharged into the condenser under emergency shutdown condition, the steam quality is higher, thus the condenser pressure and hot well water enthalpy increase accordingly. Therefore, temperature and pressure reducing device could be installed at the steam discharge outlet, to avoid condenser damage. The large volume and thermal inertia of condenser suppresses pressure increasing, as shown in Fig. 10.

The outlet pressure of the water supply system is inversely proportional to the flow rate, while the power of the feed water pump is proportional to the flow rate(see Fig. 11).

For the flow rate boundary, whether the flow rate exceeds the operating limit provides a basis for the valve control strategy optimization(see Fig. 12).

The flow rate fluctuates largely during regulating valves with regard to the pressure boundary; the pressure fluctuate greatly under the flow rate boundary. These fluctuations could be eliminated by further optimizing the valve closing curve. In a nuclear power plant, the flow and pressure at the inlet of secondary circuit usually change together. Therefore, the actual fluctuation of flow rate and pressure might be smaller than calculated results.

**Table 1**
Interface parameters for various pipeline.

| Pipeline Data | R–S | | S-R | | R | |
|---|---|---|---|---|---|---|
| | In(E) | Out(L) | In(E) | Out(L) | In(E) | Out(L) |
| Input | $p_E$ $h_E$ | $G_L$ | $G_E$ $h_E$ | $p_L$ | $p_E$ $h_E$ | $p_L$ |
| Output | $G_E$ | $p_L$ $h_L$ | $p_E$ | $G_L$ $h_L$ | $G_E$ | $G_L$ $h_L$ |

### 4.3. System overload test

For the main steam turbine overspeeding condition, the steam turbine regulating valve is opened, thus the flow rate, turbine power and speed increase. Pressure is employed as the inlet boundary condition (see Fig. 13).

With more steam entering the condenser increases, the condenser pressure rises. As shown in Fig. 14, the speed and power of turbine decrease after a rise, due to the growth of condenser pressure.

Because the initial pressure of the regulating stage steam chamber is small, the sudden change of the flow rate in the secondary circuit system are also caused by the rapid increase of flow rate (Fig. 15). Overload conditions are at the expense of steam quality, hence it should not be lasted for long periods of time.

The secondary system simulation helps to determine the regulation mode of steam system under variable working conditions. The parameter transients were analyzed under both pressure boundary and flow rate boundary. In practical nuclear power plants, the pressure and enthalpy (temperature) of steam are usually used as the regulated quantities by controling the steam flow rate in feedwater system. Hence the system stability was evaluated.

## 5. Conclusion

The transient conditions of typical secondary circuit in nuclear power plant have been analyzed in this study. The dynamic models of whole secondary circuit has been established in this study. The system response and characteristics have been investigated based on the parameter transients under emergency shutdown and overload. The following conclusions have been drawn:

Appropriate modeling methods are employed according to different processes of working fluid and energy transfer. Both compressible fluid flow and incompressible fluid flow have been considered, which are modeled by modular modeling and fluid network, respectively; the heat transfer process and the mechanical energy transfer process are modularized.

Models of main equipment have been established, including main turbine, condenser, steam pipe and feedwater system The turbine model considered various operating conditions like emergency shutdown and overspeed; condenser model could simulate abnormal operating conditions of high water level and ejector failures, and operating indicators have been obtained; steam pipelines enabled tracking flow rate and node pressures under pressure boundary; the water supply system model simulated the

**Table 2**
Comparison of this model with design value.

| Parameter | Turbine | | | Condenser | | |
|---|---|---|---|---|---|---|
| | Outlet pressure ( Mpa ) | Outlet temperature ( K ) | Inlet flow Rate ( kg/s ) | Outlet pressure ( Mpa ) | Outlet temperature ( K ) | Inlet flow rate ( kg/s ) |
| Error | 0.62% | 0.62% | 0.12% | 12.14% | 0.32% | 0 |

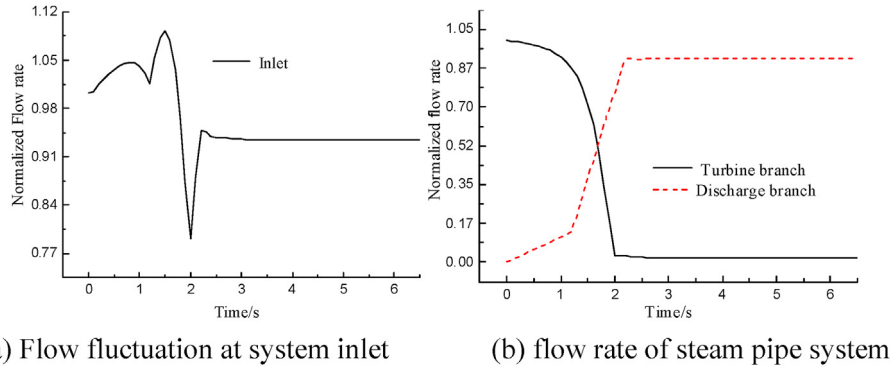


(a) Flow fluctuation at system inlet (b) flow rate of steam pipe system

**Fig. 8.** Flow rate transient of system.

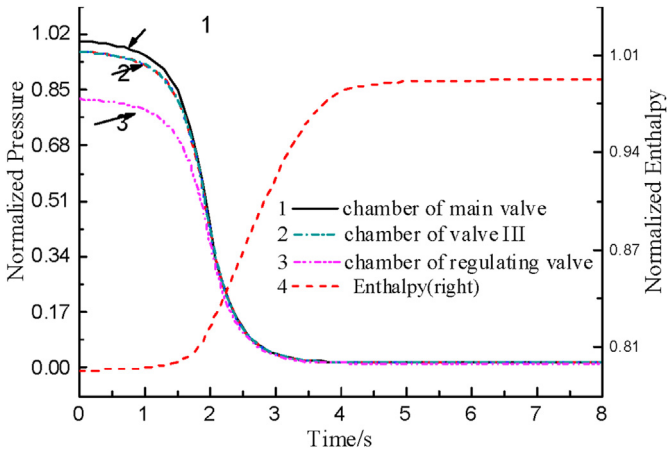


**Fig. 9.** Parameter transients of turbine.

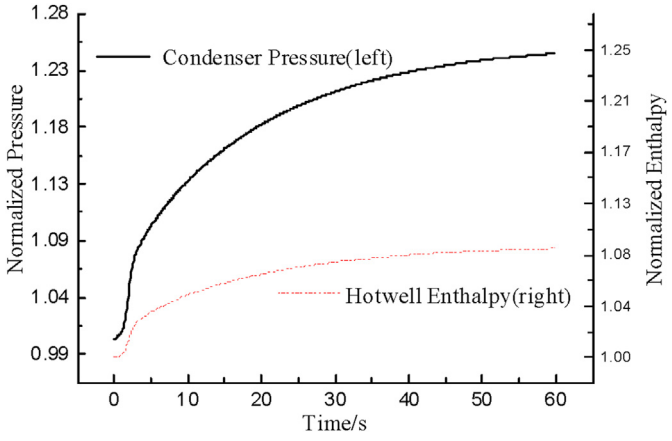


**Fig. 10.** Parameter transients of condenser.

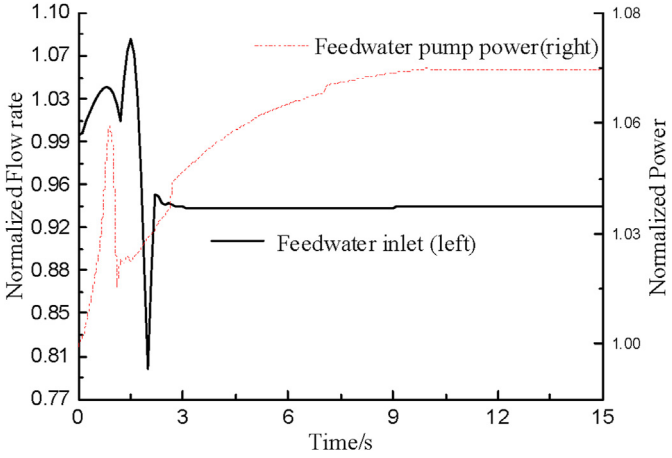


**Fig. 11.** Parameter transients of feedwater system.

(2) Flow rate boundary

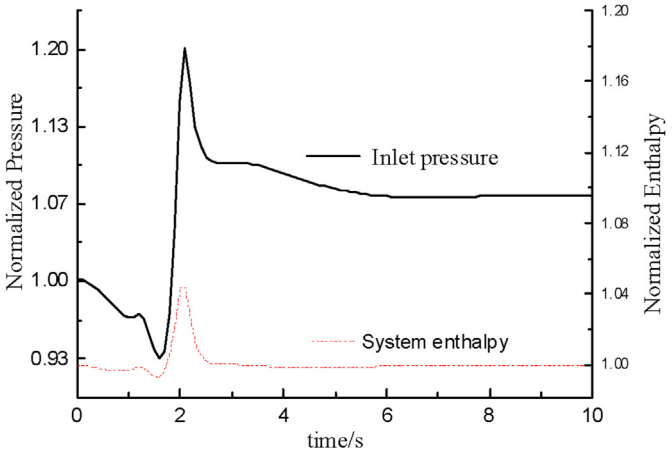


**Fig. 12.** Parameter transients under flow rate boundary.

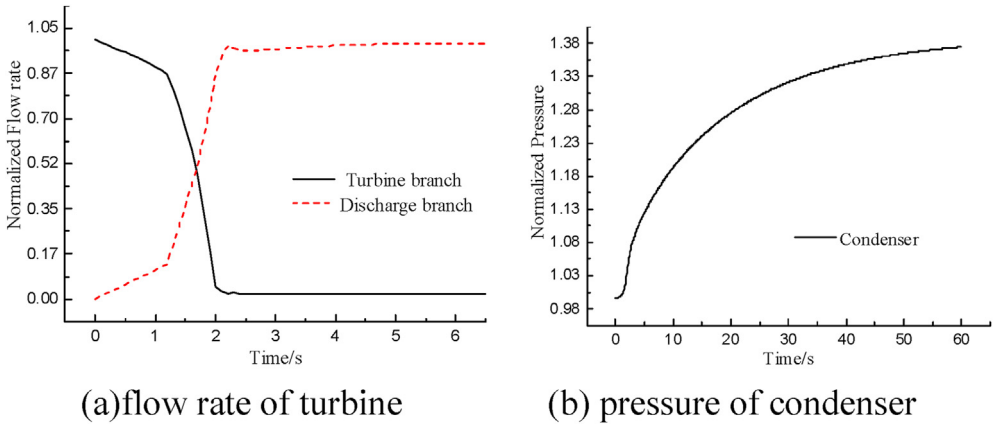


**Fig. 13.** Parameter transients of turbine and condenser.

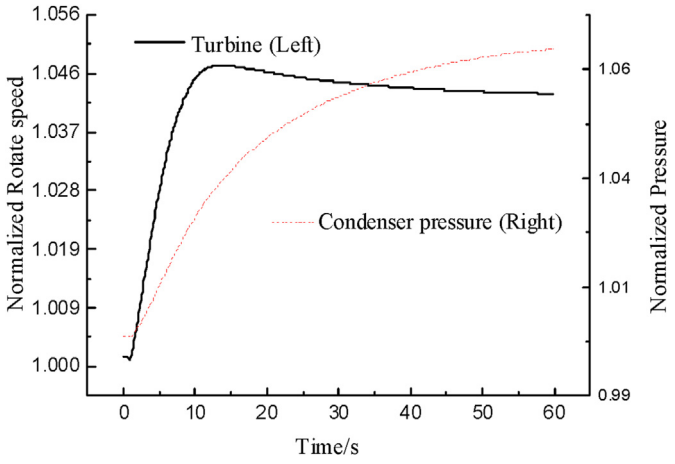


**Fig. 14.** Parameter transients of turbine and condenser.

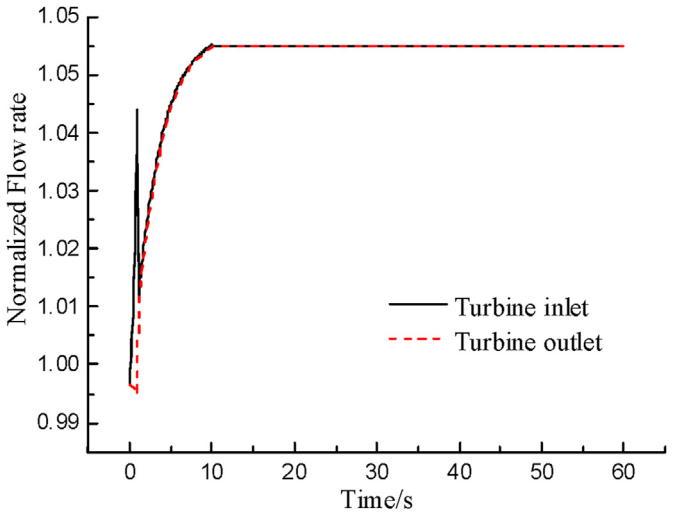


**Fig. 15.** Flow rate of system.

change of system pressure over flow rate.

The above established models have been verified by design value. The second circuit system features compressibility, high transport speed of mass and energy, strong system rigidity. The simulation of the secondary circuit system has been conducted based on the verified models, where various system characteristics have been obtained under different boundary conditions. The secondary circuit system ensures sufficient design margin to withstand the pressure and flow fluctuations. The adjustment of exhaust valve group could maintain the system pressure within a safe range, at the expense of steam quality. The condenser could rapidly take out most heat to avoid overpressure.

## Declaration of competing interest

The authors declare that they have no known competing financial interests or personal relationships that could have appeared to influence the work reported in this paper.

## Acknowledgement

The authors appreciate the support from National Natural Science Foundation of China (Grant No. 11905168) and China Postdoctoral Science Foundation (Grant No. 2018M643644).

## References

[1] T.S. Kim, H.J. Park, S.T. Ro, Characteristics of transient operation of a dual-pressure bottoming system for the combined cycle power plant[J], Energy 26 (10) (2001) 905–918.
[2] A. Elshahat, T. Abram, J. Hohorst, et al., Simulation of the westinghouse AP1000 response to SBLOCA using RELAP/SCDAPSIM, International Journal of Nuclear Energy 2014 (2014) 1–9.
[3] J. Pack, Z. Fu, F. Aydogan, Modeling primary and secondary coolant of a nuclear power plant system with a unique framework(MCUF), Prog. Nucl. Energy 83 (2015) 197–211.
[4] N.E. Todreas, S. Kazimi M, Nuclear System I Thermal Hydraulic Fundamentals, HEMISPHERE PUBLISHING CORPORATION, 1989.
[5] T.T.H. Group, SCIENTECH, Inc. RELAP5/MOD3 CODE MANUAL, vol. I, 1998.
[6] P. Colonna, Modeling of Energy Conversion Systems at TU Delft[C]. Process and Energy Department, Energy Technology Section, Delft University of Technology, 2005.
[7] P. Fritzson, Principles of Object-Oriented Modeling and Simulation with Modelica 2.1, John Wiley & Sons, 2010.
[8] S. Dai, M. Peng, Z. Tian, et al., Study on turbine simulation model based on RELAP5, Atomic Energy Sci. Technol. 47 (10) (2013) 1799–1805.
[9] P. Colonna, H. van Putten, Dynamic modeling of steam power cycles. Part I-Modeling paradigm and validation[J], Appl. Therm. Eng. 27 (2–3) (2007) 467–480.
[10] J. Zhang, M.J. Wang, Z. Zhang, et al., A comprehensive review of the leak flow through micro-cracks (in LBB) for nuclear system: morphologies and thermal-hydraulic characteristics[J], Nucl. Eng. Des. 362 (2020) 110537.
[11] H. Van Putten, P. Colonna, Dynamic modeling of steam power cycles: Part II - simulation of a small simple Rankine cycle system[J], Appl. Therm. Eng. 27 (14–15) (2007) 2566–2582.
[12] A. Jomartov, Z.G. Ualiyev, Method of Dynamic Analysis of Mechanisms of Variable Structure, 2008, pp. 329–335.

[13] F. Takahashi, I. Harada, A Computational Method for Compressible Flows with Condensation in Power Plant Condensers[M]. Challenges of Power Engineering and Environment, Springer Berlin Heidelberg, 2007, pp. 417–421.
[14] K.S.S. Raj, Deviations in predicted condenser performance for power plants using HEI correction factors: a case study[J], J. Eng. Gas Turbines Power 130 (2) (2008) 23003–23008.
[15] Q. Liu, Z. Zhang, J.H. Pan, et al., A coupled thermo-hydraulic model for steam flow in pipe networks[J], J. Hydrodyn. 21 (6) (2009) 861–866.
[16] Y. Zhang, W. Tian, S. Qiu, et al., Transient analyses of station blackout accident for CPR1000, Atomic Energy Sci. Technol. 45 (9) (2011) 1056–1059.
[17] W.W. Wang, W.X. Tian, G.H. Su, et al., Development of a thermal-hydraulic safety analysis code RETAC for AP1000, Prog. Nucl. Energy 55 (2012) 49–60.